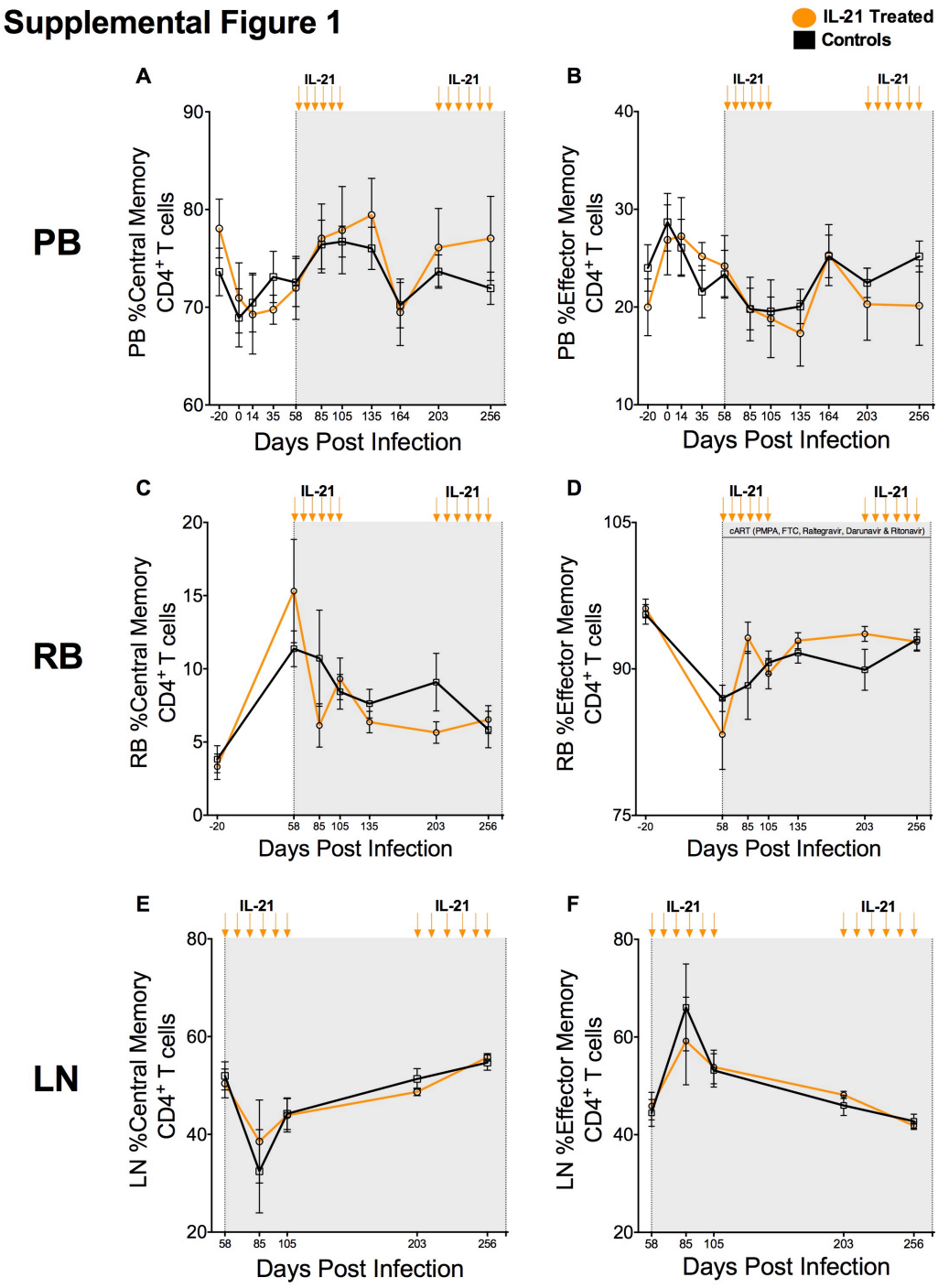

Supplemental Figure 1. **Effects of IL-21 treatment on memory CD4$^+$ T-cell subsets**. Longitudinal assessment of the fractions of CD4$^+$ T-cells with a central memory (CD28$^+$CD95$^+$CCR7$^+$; **A,C,E**) or effector memory (CD28$^+$CD95$^+$CCR7$^-$; **B,D,F)** phenotype in peripheral blood (PB; **A,B)**, colorectal (RB; **C,D**), and lymph node (LN; **E,F**). IL-21 treated animals (n=7) are depicted as (●), controls (n=8) as (■). Shaded area represents time of ART treatment and orange arrows represent IL-21 administrations. Averaged data are presented as mean ± SEM.

Supplemental Figure 2

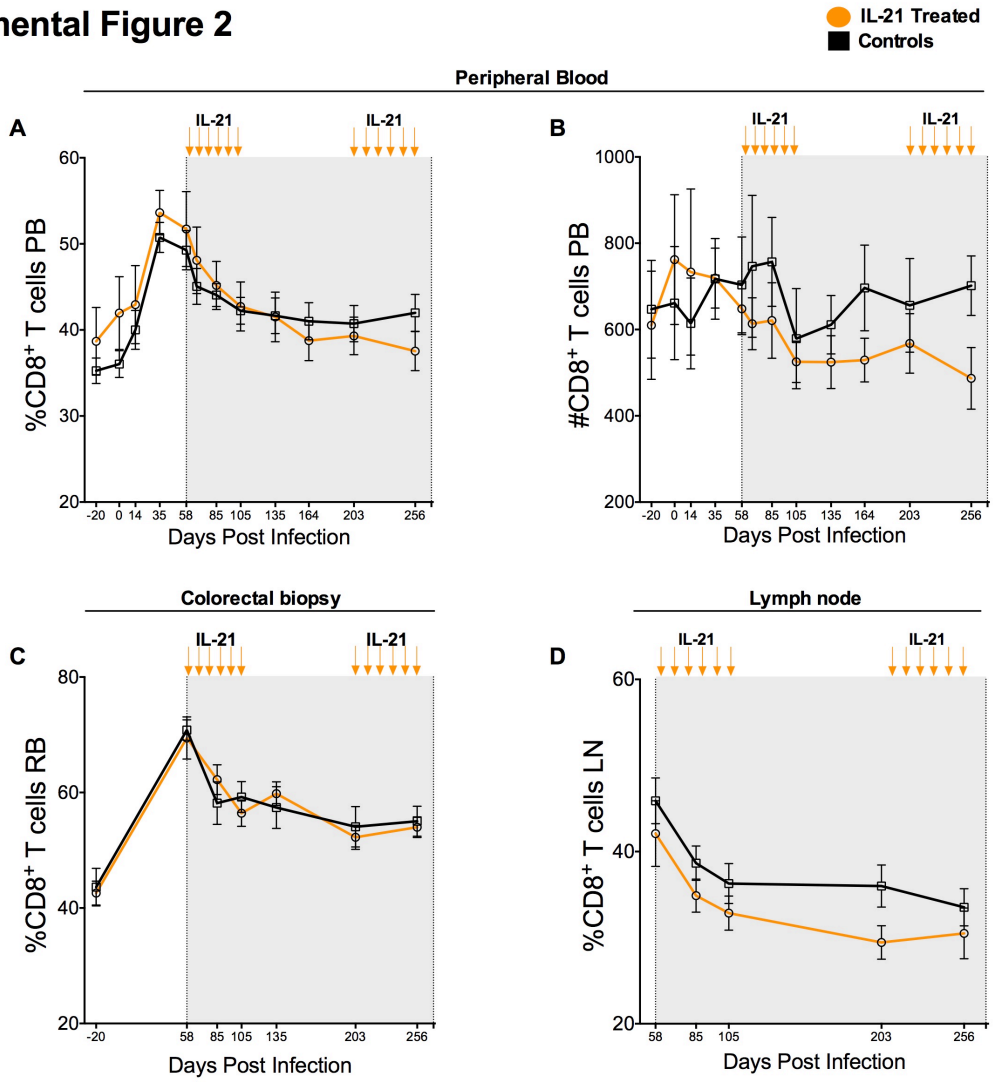

Supplemental Figure 2. Effects of IL-21 treatment on CD8$^+$ T-cell levels. Longitudinal assessment of the frequencies (**A**) and absolute counts (cells per µl of blood; **B**) of peripheral blood (PB) CD8$^+$ T-cells. Frequencies of CD8$^+$ T-cells were also determined in colorectal (RB; **C**), and lymph node (LN; **D)** biopsies. IL-21-treated animals (n=7) are depicted as (●), controls (n=8) as (■). Shaded area represents time of ART treatment and orange arrows represent IL-21 administrations. Averaged data are presented as mean ± SEM.

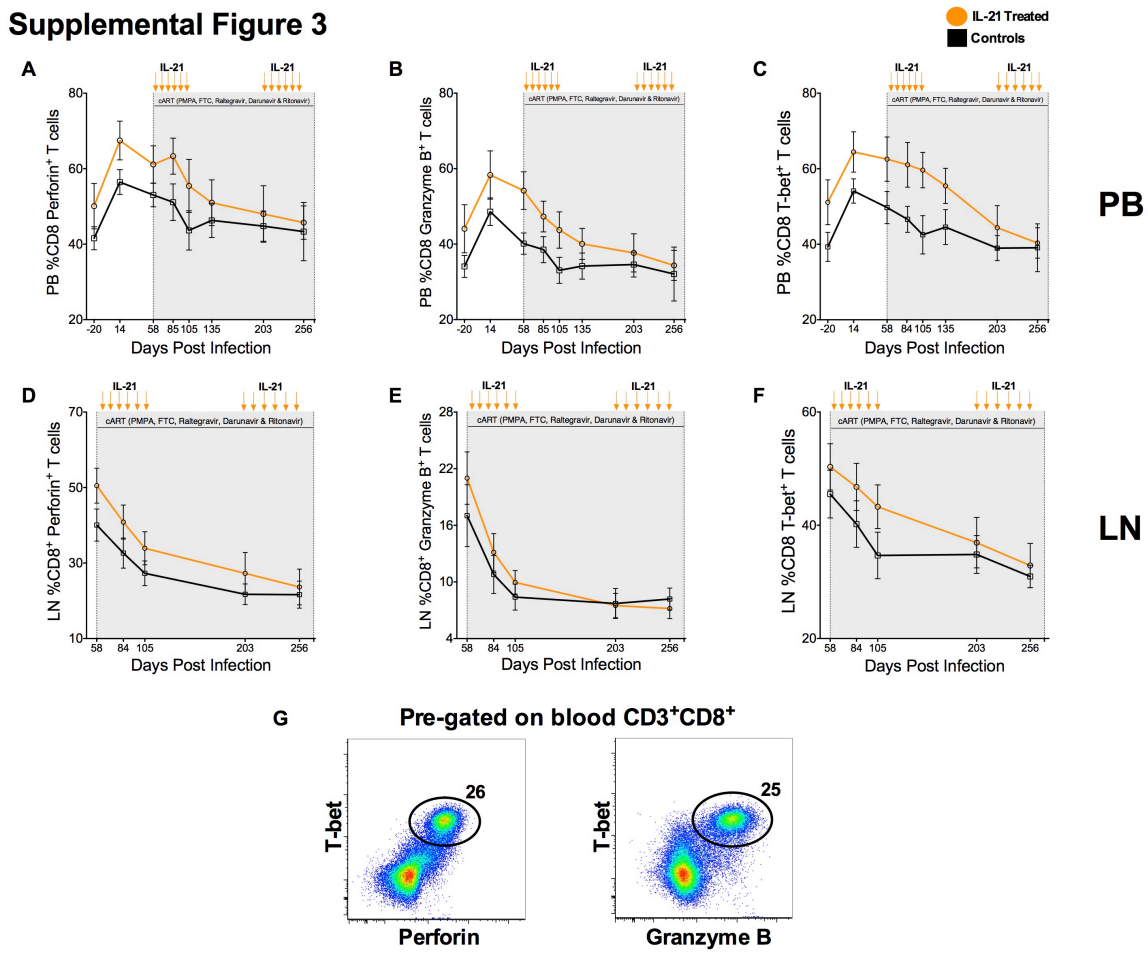

Supplemental Figure 3. Effects of IL-21 treatment on the frequencies of CD8$^+$ T-cells expressing perforin, granzyme B, and T-bet. Longitudinal assessment of the frequencies of peripheral blood (**A-C**) and LN (**D-F**) CD8$^+$ T-cells expressing perforin (**A,D**), granzyme B (**B,E**), or T-bet (**C,F**). (**g**) Representative staining for T-bet by perforin and T-bet by granzyme B in blood CD3$^+$CD8$^+$ T-cells from a representative IL-21-treated RM at d105 p.i. IL-21-treated animals (n=7) are depicted as (●), controls (n=8) as (■). Shaded area represents time of ART treatment and orange arrows represent IL-21 administrations. Averaged data are presented as mean ± SEM.

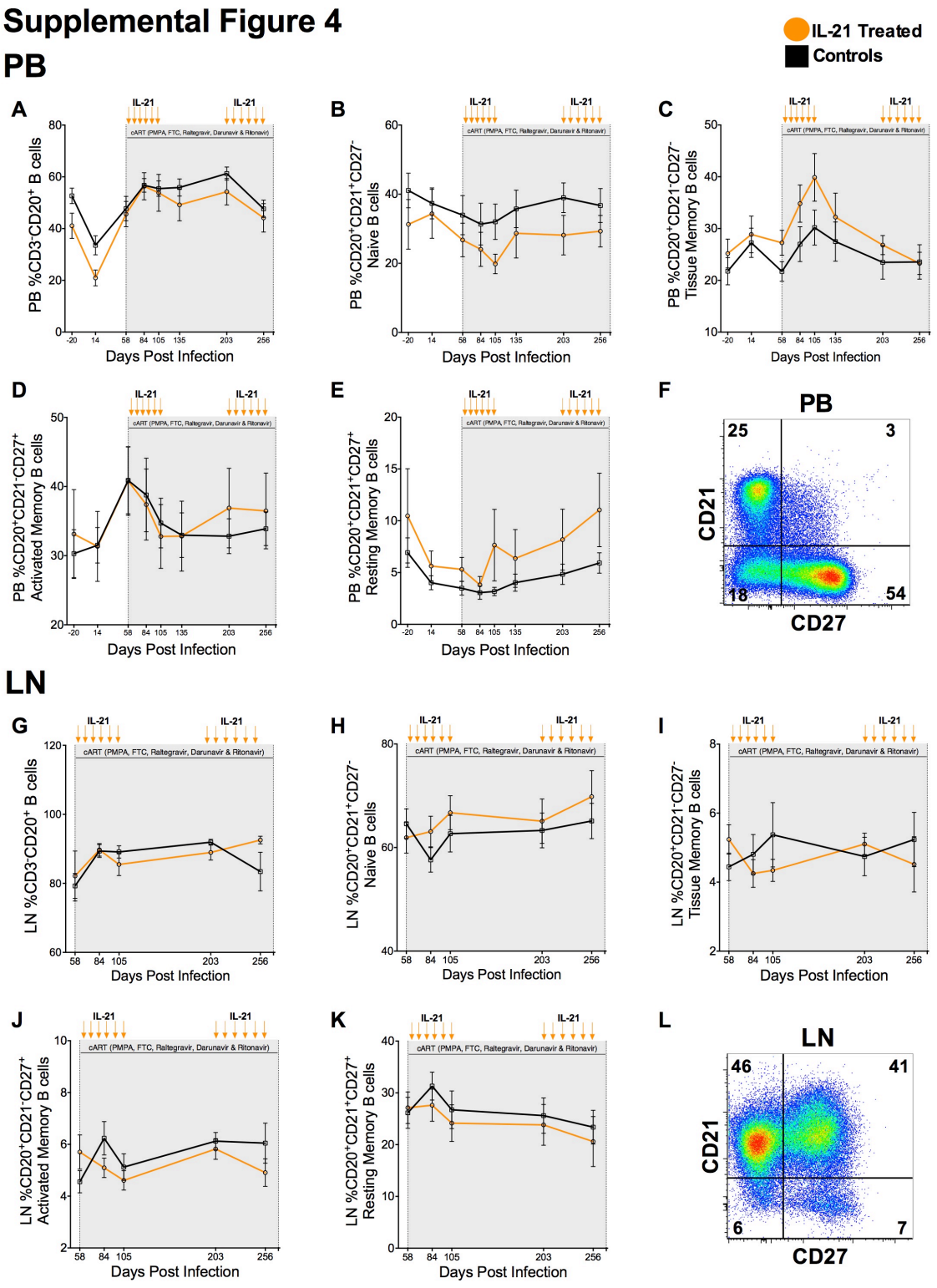

Supplemental Figure 4. Effects of IL-21 treatment on blood and LN B-cell levels. Longitudinal assessment of the percentages of blood (**A-E**) and LN (**G-K**) $CD3^{-}CD20^{+}$ B-cells (**A,G)** as well as their naïve (CD21+CD27-; **B,H**), tissue memory (CD21-CD27-;

C,I) activated memory (CD21-CD27+; **D,J**), and resting memory (CD21+CD27+; **E-K**) subsets. (**F,L**) Representative staining for CD21 by CD27 in $CD3^{-}CD20^{+}$ B-cells from a representative IL-21-treated RM at d105 p.i. IL-21 treated animals (n=7) are depicted as (●), controls (n=8) as (■). Shaded area represents time of ART treatment and orange arrows represent IL-21 administrations. Averaged data are presented as mean ± SEM

Supplemental Figure 5

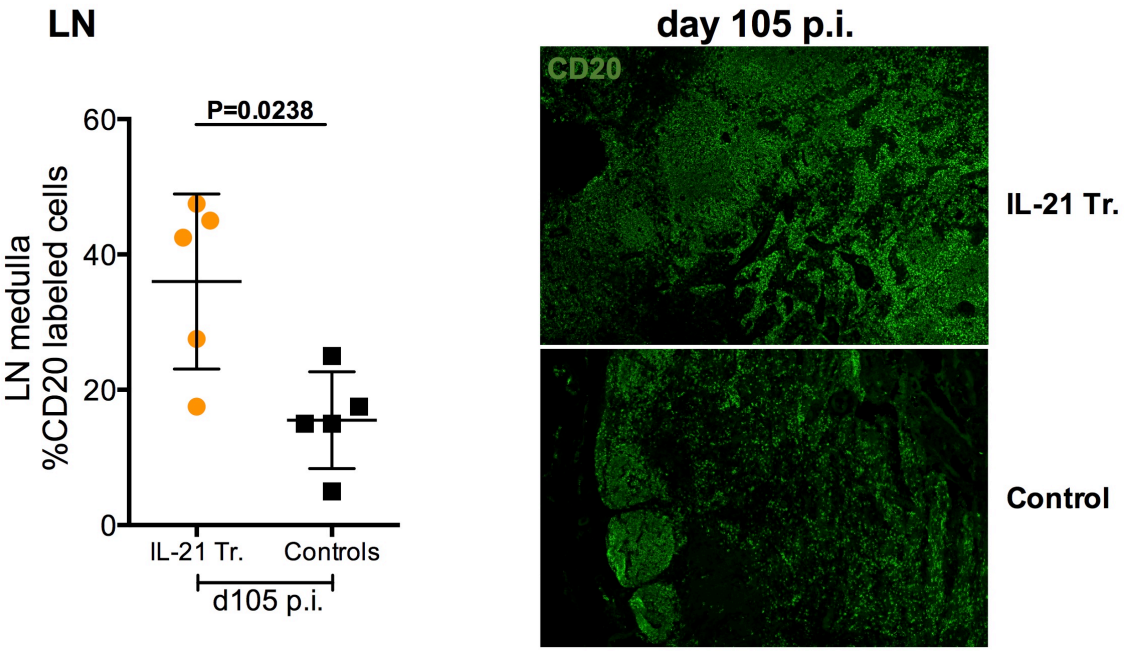

Supplemental Figure 5. Effects of IL-21 treatment on the localization of B-cells in the LN. IHC analyses on LN biopsies showed that early on-ART IL-21-treated animals have higher levels of B-cells in the medulla when compared to controls (P=0.0238; n=5). Random 20× and 200× images of LN were taken and the percent area staining for CD20 was determined in IL-21-treated (n=5) (●) and control (n=5) (■) RMs (left). The right panels show a representative CD20 staining (200×) in one IL-21-treated (top panel) and one control (bottom panel) RM on-ART (d105 p.i.). Statistical analysis was performed by Mann-Whitney t-test.

Supplemental Figure 6

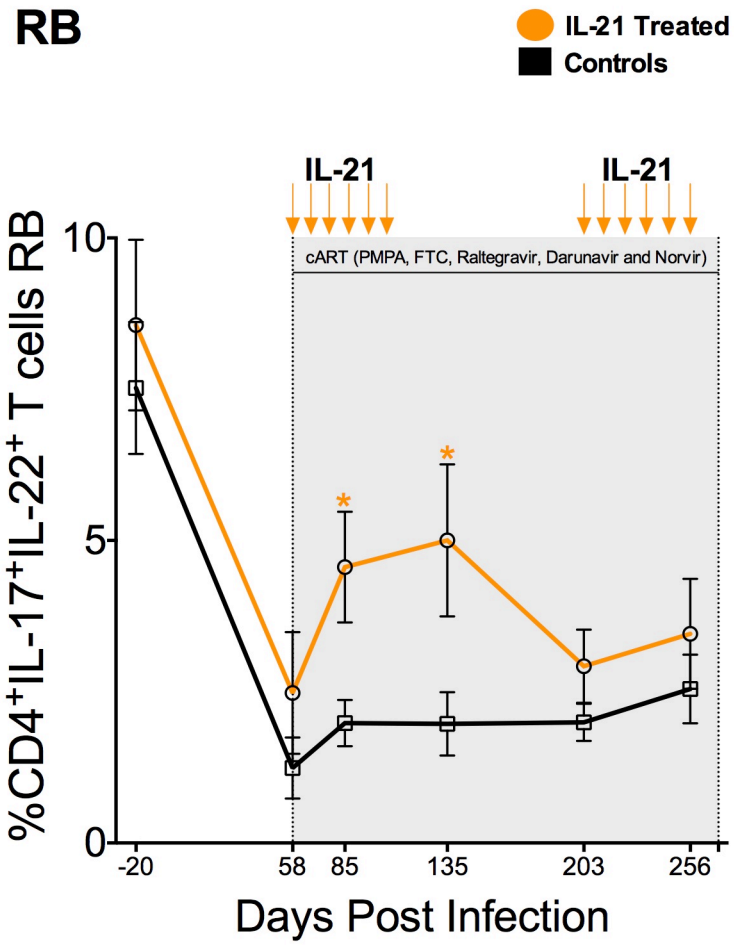

Supplemental Figure 6. Higher levels of intestinal CD4$^+$ T-cells co-expressing IL-17 and IL-22 in IL-21-supplemented RMs. Longitudinal assessment of the frequency of intestinal CD4$^+$ T cells producing IL-17 and IL-22. The levels of CD4$^+$IL-17$^+$IL-22$^+$ T-cells were significantly higher in the rectum of IL-21-treated (n=7) RMs (●) as compared to controls (n=8) (■) at d85 and 135 p.i. (P=0.0209 and P=0.0281, respectively). Shaded area represents time of ART treatment and orange arrows represent IL-21 administrations. Averaged data are presented as mean ± SEM. Repeated-measures analyses were performed with a means model (SAS Proc Mixed v9) to generate statistical outcomes.

Supplemental Figure 7

LN

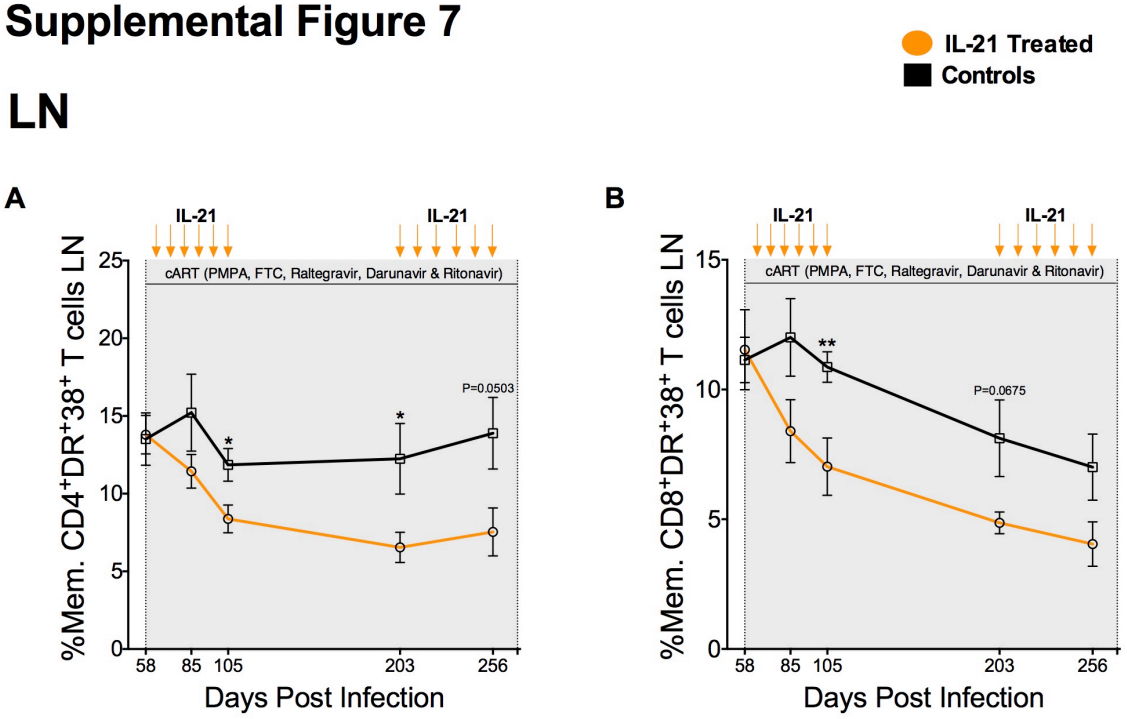

Supplemental Figure 7. Effects of IL-21 treatment on T-cell activation in the LN. Longitudinal assessment of the frequencies of LN-derived memory $CD4^+$ (**A**) and $CD8^+$ (**B**) T-cells expressing the activation markers HLA-DR^+CD38^+. IL-21-treated animals (n=7) are depicted as (●), controls (n=8) as (■). Shaded area represents time of ART treatment and orange arrows represent IL-21 administrations. Averaged data are presented as mean ± SEM. Repeated-measures analyses were performed with a means model (SAS Proc Mixed v9) to generate statistical outcomes.

Supplemental Figure 8

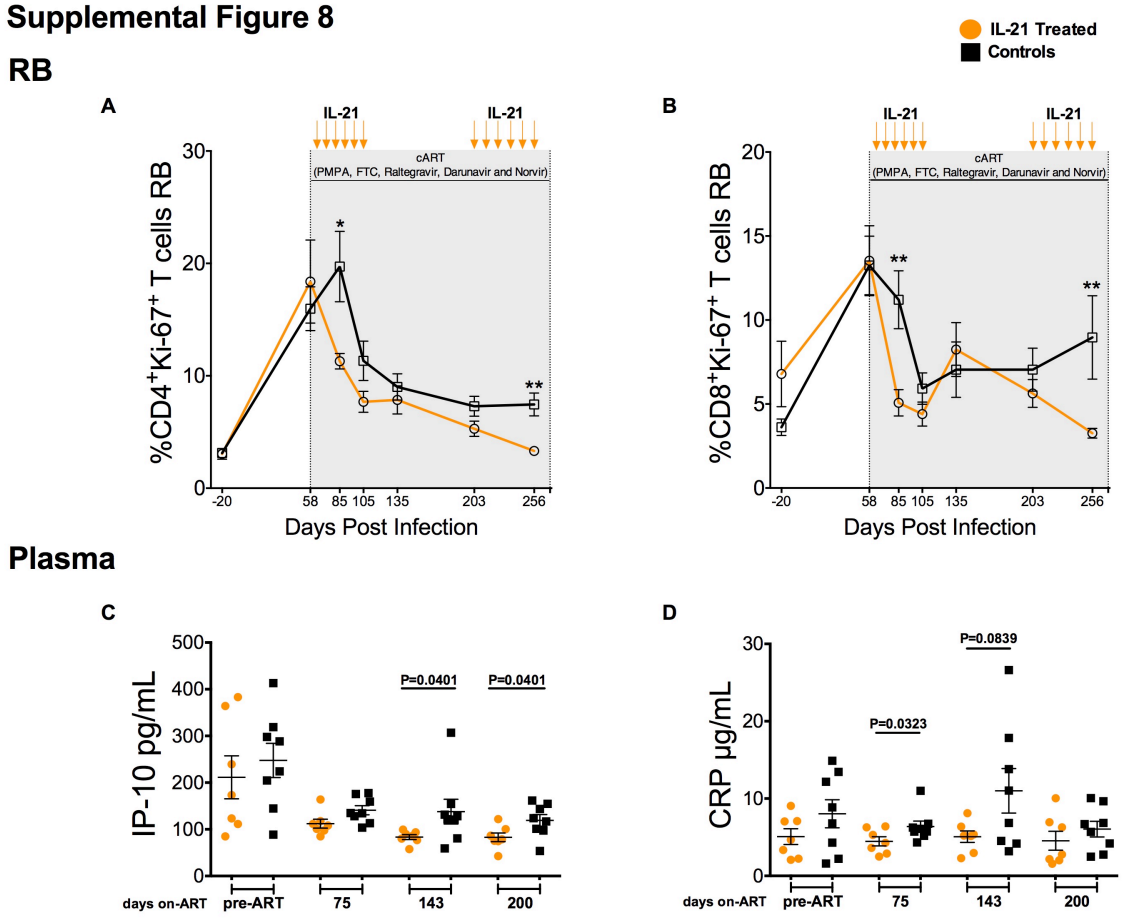

Supplemental Figure 8. Reduced levels of intestinal T-cell proliferation and soluble markers of inflammation in IL-21-treated RMs. (A,B) Longitudinal assessment of the frequencies of intestinal $CD4^+$ (**A**) and $CD8^+$ (**B**) T-cells expressing the proliferation marker Ki-67 in IL-21-treated (n=7) (●) and control (n=8) (■) RMs. Fractions of proliferating $CD4^+$ and $CD8^+$ T-cells were significantly lower in the rectum of IL-21-treated animals at d85 and 256 p.i. Shaded area represents time of ART treatment and orange arrows represent IL-21 administrations. Averaged data are presented as mean ± SEM. (**C,D**) Plasma levels of IP-10 (**C**) and CRP (**D**) were compared between IL-21-treated and control RMs at pre-ART and different experimental points on-ART. Although similar to those found in controls at pre-ART, IL-21-treated RMs showed significantly lower levels of IP-10 at d143 and d200 on-ART (P=0.0401 for both experimental points) and of CRP at d75 on-ART (P=0.0323). Averaged data are presented as mean ± SEM. Repeated-measures analyses were performed with a means model (SAS Proc Mixed v9) to generate statistical outcomes.

Supplemental Figure 9

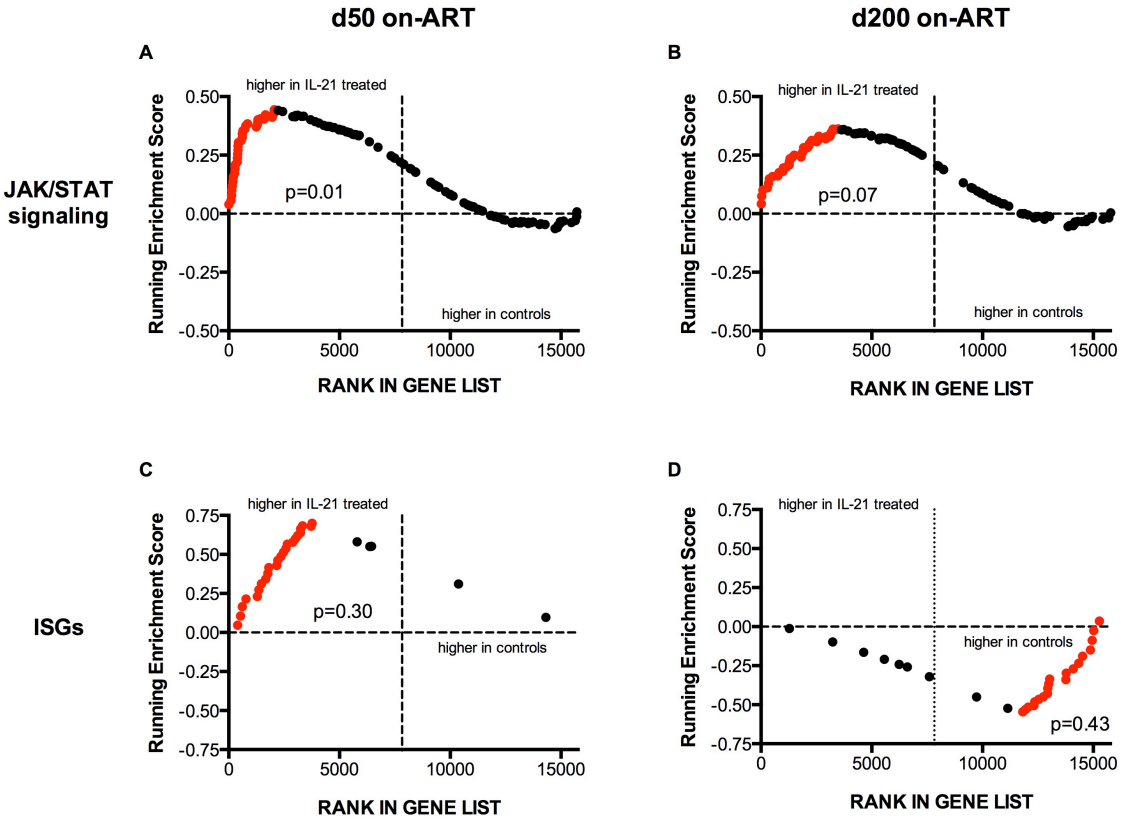

Supplemental Figure 9. GSEA analysis of enriched pathways in IL-21-treated versus control RMs. Representation of the rank in gene list of JAK/STAT pathway at d50 (**A**) and d200 (**B**) on-ART, as well as for interferon-stimulated genes (ISGs) at d50 (**C**) and d200 (**D**) on-ART. Leading genes with higher enrichment score are depicted as (●). Statistical analyses were performed with GSEA tool.

Supplemental Figure 10

Rectal Biopsy

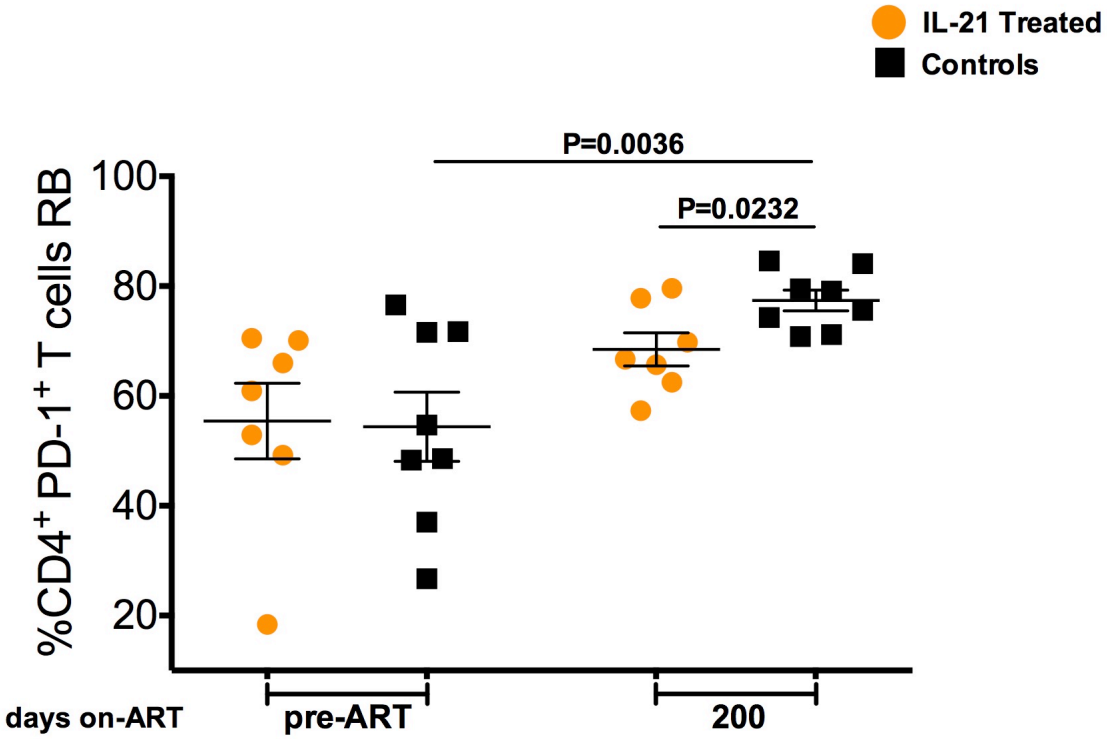

Supplemental Figure 10. Reduced levels of $CD4^+$ $PD\text{-}1^+$ T-cells in the rectum of IL-21-treated RMs. Fractions of intestinal $CD4^+$ T-cells expressing PD-1 were longitudinally determined throughout the study. Although similar (or even higher) to those found in controls at pre-ART, the fractions of $CD4^+$ $PD\text{-}1^+$ T-cells at d200 on-ART were significantly lower (P=0.0232) in IL-21 supplemented RMs. IL-21-treated animals (n=7) are depicted as (●), controls (n=8) as (■). Averaged data are presented as mean ± SEM. Repeated-measures analyses were performed with a means model (SAS Proc Mixed v9) to generate statistical outcomes.

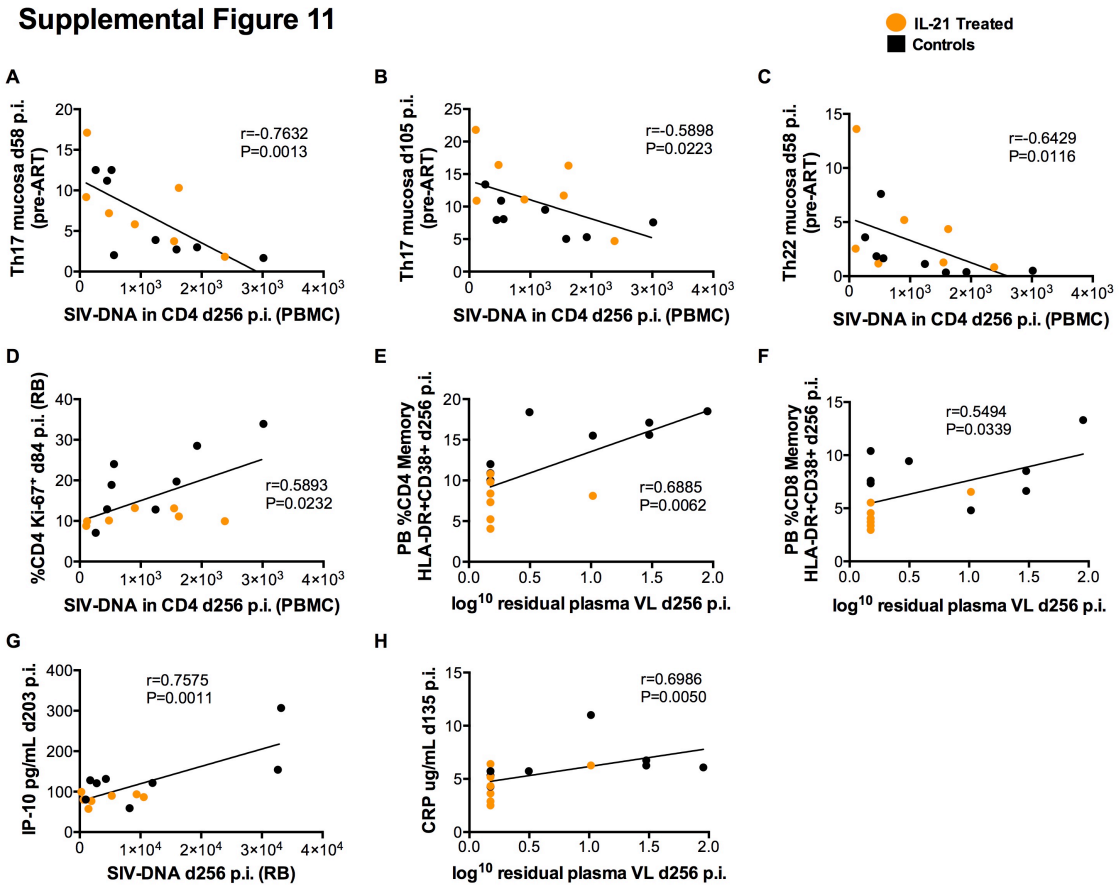

Supplemental Figure 11. Markers of mucosal immunity and inflammation correlate with measures of SIV persistence. SIV-DNA content in purified blood $CD4^+$ T-cells at the latest time point on-ART (d256 p.i.) correlates negatively with the levels of intestinal Th17 (**A**) and Th22 cells (**C**) at pre-ART, negatively with the levels of intestinal Th17 cells on-ART (**B**), and positively with the levels of intestinal $CD4^+Ki\text{-}67^+$ T-cells on-ART (**D**). At the latest time point on-ART, the levels of activated (HLA-DR+CD38+) circulating $CD4^+$ (**E**) and $CD8^+$ (**F**) T-cells positively correlate with residual plasma viremia. Plasma levels of IP-10 (**G**) and CRP (**H**) on-ART positively correlate with SIV-DNA content in intestinal tissues and residual plasma viremia, respectively. IL-21-treated animals (n=7) are depicted as (●), controls (n=8) as (■).

Supplemental Figure 12

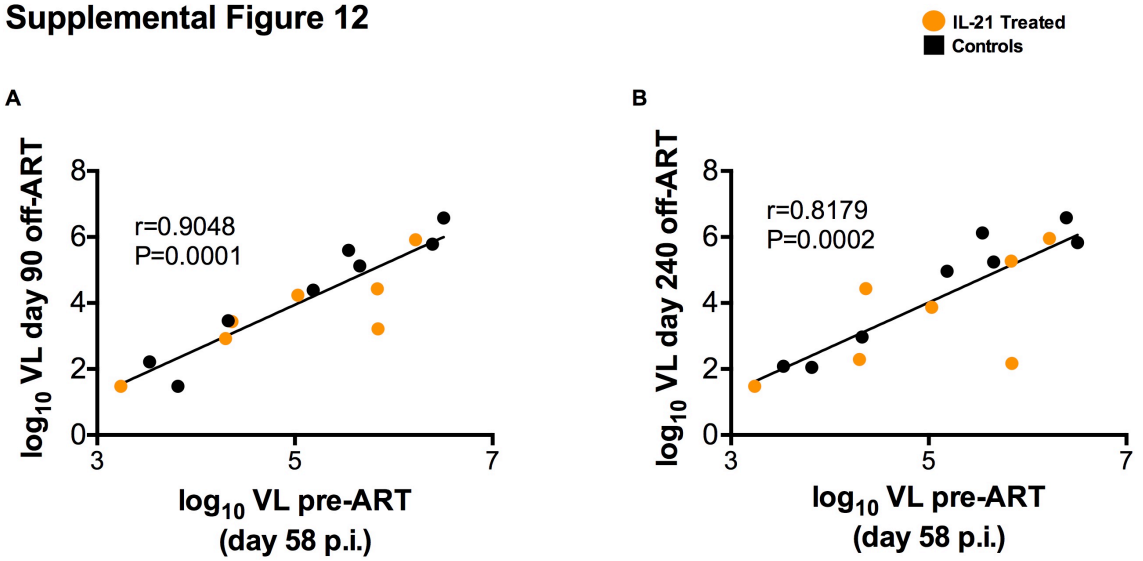

Supplemental Figure 12. Pre-ART plasma viremia strongly correlates with viral rebound post-ART interruption. Plasma viremia at pre-ART (d58 p.i.) positively correlates with plasma viremia at days 90 (**A**) and 240 (**B**) post-ART interruption. IL-21-treated animals (n=7) are depicted as (●), controls (n=8) as (■).

Supplemental Figure 13

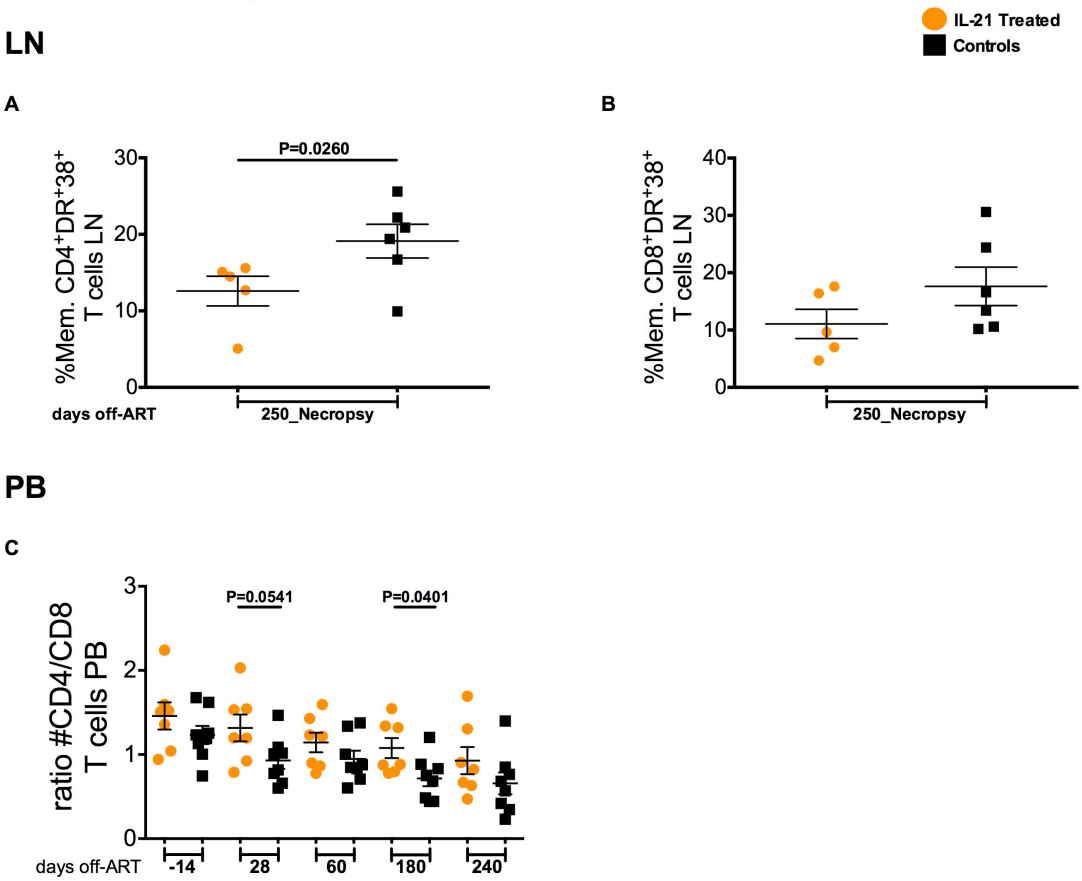

Supplemental Figure 13. Reduced lymph node T-cell activation and higher blood CD4$^+$ to CD8$^+$ T-cell ratios in IL-21-treated RMs following ART interruption. (**A,B**) Fraction of lymph node derived CD4$^+$ (**A**) and CD8$^+$ (**B**) T-cells expressing HLA-DR and CD38 at necropsy (d250 off-ART). T cell activation levels were lower in IL-21-treated (n=5-7) RMs (●) as compared to controls (n=6-8) (■), with the differences reaching statistical significance for CD4+ T-cells, (P=0.0260). (**C**) The ratios between the absolute counts of blood CD4$^+$ and CD8$^+$ T-cells were longitudinally compared between IL-21-treated and control RMs. CD4$^+$ to CD8$^+$ T-cell ratios were higher in IL-21-treated RMs, with the differences reaching statistical significance at d180 off-ART (P=0.0401). Averaged data are presented as mean ± SEM. Repeated-measures analyses were performed with a means model (SAS Proc Mixed v9) to generate statistical outcomes.

Supplemental Table 1

Animal ID	Age	Sex	#CD4 preART	VL preART	MamuA01 genotype	IL-21 Tx	Diarrhea Rx	Anemia Rx	Weight loss*
RLm12	57 ms	F	540	1.07E+05	+	y	n	n	y
ROe12	65 ms	F	707	1.73E+03	-	y	n	y	n
RJp11	81 ms	F	709	1.99E+04	+	y	n	n	y
RGv10	102 ms	F	379	6.94E+05	-	y	n	y	y
RVt10	98 ms	F	366	6.83E+05	+	y	n	n	n
RTb12	71 ms	F	364	1.66E+06	-	y	n	y	y
ROc10$^{\Psi}$	114 ms	F	209	1.27E+06	+	y	n		
RHa10	114 ms	F	618	2.31E+04	-	y	n	y	n
RBt12	57 ms	F	678	6.56E+03	+	n	n	y	y
RGe12	67 ms	F	594	3.20E+06	-	n	n	n	n
RCb12	70 ms	F	942	3.38E+03	+	n	n	n	y
RJw12	54 ms	F	463	4.54E+05	-	n	n	n	y
RKg11	90 ms	F	1108	2.12E+04	+	n	n	n	y
RPu12	57 ms	F	280	2.47E+06	-	n	n	y	y
RKd12	68 ms	F	452	1.53E+05	-	n	n	y	y
RPy8	120 ms	F	374	3.50E+05	+	n	n	y	n

Animals included in the study. $^{\Psi}$ ROc10 died at d140 p.i; **ms** (months) at time of infection; **F** (Female); **#CD4 pre-ART** in blood (cells/µL); **V**iral **L**oad **pre-ART** (day 58 p.i.), SIV-RNA copies/mL of plasma; **+** (positive) and **–** (negative); **y** (yes) and **n** (no); ***** weight loss above 10% of the pre-infection weight. All RMs were treated with ART.

Supplemental Table 2

Immunologic and virologic markers	Day p.i.	Tissue	Related gene	Correlation r values
Memory %CD4 HLA-DR+CD38+	Day 105	Colorectal biopsy	**PRDM1**	-0.514763
			SOCS1	-0.700644
			IL22	-0.602942
Memory %CD4 HLA-DR+CD38+	Day 256	Colorectal biopsy	**SOCS1**	-0.536038
			MUC4	-0.601547
			TLR7	0.618818
			IL17F	-0.597841
Memory %CD8 HLA-DR+CD38+	Day 105	Colorectal biopsy	**PRDM1**	-0.520453
			SOCS1	-0.587045
Memory %CD8 HLA-DR+CD38+	Day 256	Colorectal biopsy	**TLR7**	0.743636
			IL17F	-0.72236
%CD4 Ki-67+	Day 105	Colorectal biopsy	**PRDM1**	-0.551366
			IL23R	-0.595036
%CD4 Ki-67+	Day 256	Colorectal biopsy	**AHR**	-0.527883
%CD8 Ki-67+	Day 105	Colorectal biopsy	**SOCS3**	-0.528842
			PTGS2	-0.517683
			S100A8	-0.497802
%CD8 Ki-67+	Day 256	Colorectal biopsy	**AHR**	-0.590169
			CAMP	-0.518008
			TREM1	-0.575188
			CCR2	-0.575164
LP %PMN_MPO	Day 105	Colorectal biopsy	**SOCS3**	-0.565448
			PTGS2	-0.640115
			S100A8	-0.568288
%CD4 IL-17+	Day 105	Colorectal biopsy	**SOCS1**	0.690619
			TNF	-0.57258
			PRDM1	0.536043
%CD4 IL-22+	Day 256	Colorectal biopsy	**IL23R**	0.727713
			IL6	-0.717971
			DEFA1	0.654452
			RGS18	0.554019
			IL4	0.720438
Cell-associated SIV-RNA	Day 105	Colorectal biopsy	**TREM1**	-0.555096
Memory %CD4 HLA-DR+CD38+	Day 105	Blood	**SOCS1**	-0.545821
%CD4 Ki-67+	Day 105	Blood	**IL10**	0.541909
			FOXP3	0.607558
			TNF	0.561581
			ICOS	0.578906
%CD8 Ki-67+	Day 105	Blood	**TNF**	0.599172
Cell-associated SIV-DNA in CD4+	Day 105	Blood	**SOCS3**	-0.593307
			FOXP3	0.518763
			BCL6	-0.67013
			AHR	-0.538248
			S100A8	-0.6728
			TREM1	-0.576074
			CCR2	-0.520335
Memory %CD4 HLA-DR+CD38+	Day 105	Lymph node	**SOCS1**	-0.543691
			VNN2	-0.521476

Memory %CD8 HLA-DR+CD38+	Day 105	Lymph node	**SOCS1** **IRF4**	-0.79014 -0.601648
%CD4 Ki-67+	Day 105	Lymph node	**AHR** **CCR2**	-0.599085 -0.533355
%CD4 Ki-67+	Day 256	Lymph node	**EOMES** **IRF4**	-0.711951 -0.664508
%CD8 Ki-67+	Day 105	Lymph node	**AHR** **CCR2**	-0.576554 -0.569371
%CD8 Ki-67+	Day 256	Lymph node	**EOMES**	-0.747841
Residual viral SIV-RNA	Day 105	Plasma	**IL21R**	-0.578903
Residual viral SIV-RNA	Day 256	Plasma	**CLU** **CCR2**	-0.645965 -0.591526

Immunologic and virologic markers associated with RNA-Seq transcripts. **Day p.i**; data of the experimental point used; **Tissue**; data of the anatomical compartment used; **Related gene**; RNA transcript correlated with the immunological and virologic markers; **Correlation r values**; r value of each correlation. P-value (<0.05) for all the correlations.

Supplemental Table 3

Immunologic and Virologic Markers	Day p.i.	Immunologic and Virologic Correlates	Correlation r values	P values
SIV-DNA copies in $CD4^+$ T cells (PBMC)	256 (200 on-ART)	**Log_{10} VL d58 only IL-21 Tr.**	0.6598	0.1068
		Log_{10} VL d58 only Controls	0.7022	0.0612
SIV-DNA copies (RB)	256 (200 on-ART)	**Log_{10} VL d58 only IL-21 Tr.**	0.7500	0.0663
		Log_{10} VL d58 only Controls	0.0931	0.8263
Log_{10} plasma Viral Load	58 (pre-ART)	**%$CD8^+DR^+CD38^+$ d105 (RB)**	0.2437	0.3815
		%$CD8^+DR^+CD38^+$ d256 (RB)	0.2643	0.3402
		Th17 d58 (RB)	-0.6988	0.0047
		Th17 d105 (RB)	-0.2739	0.3233
		Th22 d58 (RB)	-0.4500	0.0944
		%CD4 Ki-67^+ d84 (RB)	0.4392	0.1014
		IP-10 pg/mL d203 (plasma)	-0.2119	0.4483
		CRP ug/mL d135 (plasma)	0.3204	0.2443
		Log_{10} VL d90 off-ART	0.9048	0.0001
		Log_{10} VL d240 off-ART	0.8179	0.0002

Immunologic and virologic markers associated with pre-ART plasma viremia. **Day p.i.**; data of the experimental point used.

Supplemental Table 4

Animal ID	VL d135 p.i.	PB #CD4 d135 p.i.	PB %CD8 DR^+38^+ d135 p.i.	RB %CD4 d135 p.i.	RB %Th17 d135 p.i.	RB %Th12 d135 p.i.	RB %CD8 DR^+38^+ d135 p.i.
ROc10 [Ψ]	82	322	3.57	32.5	19.7	15.2	8.6
Av. IL-21 Tr.	30	683	4.6	21.4	13.3	7.2	7.8
Av. Controls	50	732	9.5	26.8	6.7	3.2	15.8

[Ψ] ROc10 was euthanized at day 140 p.i. and the data reported were collected at necropsy; **Av.** (average) of IL-21 treated (excluding ROc10) and control groups at day 135 p.i. (closest experimental point to ROc10's necropsy at d140 p.i.); **VL** (viral load), limit of detection 60 copies/mL of plasma; **PB** (peripheral blood); **RB** (rectal biopsy).